Wire bonding: a thorough numerical methodology

B. Carasi, L. Guarino, L. Zullino, L. Cecchetto
STMicroelectronics srl
via C. Olivetti, 2, 20864 Agrate Brianza (MB), Italy
Email: {beatrice.carasi|lucrezia.guarino|lucia.zullino|luca.cecchetto}@st.com

Abstract

The semiconductor industry is always looking for early anticipation of manufacturing risks, pushing the development of Computer Aided Engineering (CAE) modeling of processes. Robust Chip-Package Interaction (CPI) design requires a deep understanding of thermo-mechanical stresses imposed during the assembly process; one of the critical steps is wire bonding, which can damage pads inducing cracks in dielectric layers. Aim of this paper is the investigation of an appropriate simulation strategy, using COMSOL Multiphysics, of a 3D thermo-mechanical model of thermo-sonic wire bonding, that represents the physics accurately but also seeks numerical robustness, starting from appropriately simplified models. How numerical analysis together with experimental data can be used to obtain mechanical material characterization for thin/high temperature copper wires is also shown.

1. Introduction

1.1 The wire bonding process

CPI design is concerned with making sure that silicon die (the 'chip') maintains its performance when packaged. Packaging is necessary to protect the device from the environment and connect it with its application. There are many ways to achieve electrical interconnection and wire bonding (WB) is one of the alternatives (others are, for example, solder balls and direct copper interconnection). Wire bonding (see Figure 1) consists on the formation of a free air ball (FAB) at the tip of a metal wire constrained and moved by a capillary. A spark melts the wire and then the ball is pushed on the chip pad and oscillated. When the bond between ball and pad is formed the capillary lifts and translates. The wire forms a loop and then gets stitched to the package side of the connection and cut (Figure 2). This paper focuses on the first part of the process i.e. the ball-pad connection. This is the most critical one, with respect to structural assessment, since it is the die that contains functional ingredients that need to maintain their integrity during the bonding process. Also, the wire-pad interface needs to be strong enough to stay in place during operational lifetime of the chip and provide an appropriate electrical connection area. Inputs of the first bond process (and so of the numerical model) are the *temperature*, the *vertical force* on the capillary and the *ultrasonic (US) power* (combination of oscillation frequency and amplitude of the capillary tool) at each step of the process (segment). Multiple segments are possible depending on the product specifics. Many factors, including material properties of the involved surfaces [1], influence the solid state weld that is formed.

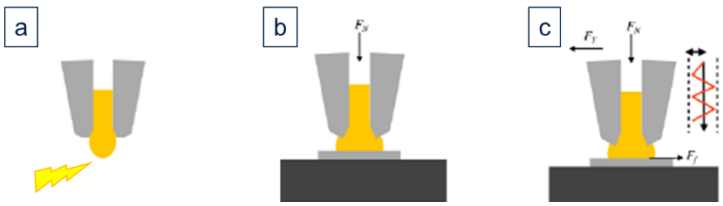

Figure 1, Wire Bonding process. 1. electrical spark, 2. vertical force application 3. ultrasonic vibration.

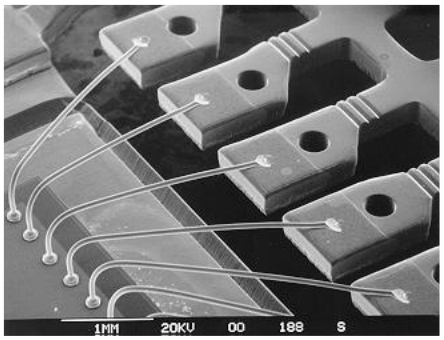

Figure 2 First (chip) and second (frame) bonds

1.2 The numerical model

The purpose of a numerical model for wire bonding is to provide feedback both to front end (chip) design and back end (packaging) process. With it, different material stacks, routing and bonding process parameters can be explored [2]. It will be shown that numerical models can be used to infer material characterization, provided that experimental data are available. Translation onto a mathematical model of the process described in chapter 1.1 can reach different degrees of accuracy (and numerical complexity). A somewhat complete description of WB would be a 3D, transient, structural mechanics model with contacts, non-linear materials, surface friction and stick criterion to describe welding, accounting for thermal gradients in the structure and, as it will be evident, a proper knowledge of the ultrasonic transducer kinematic behavior. It is well understood, in the simulation community, that a correctly simplified model can be of great insight and constitutes fundamental numerical foundation to build more complete ones.

1.2.1 Numerical models as characterization tools

Thermo-sonic wire bonding is a process in which the wire (here copper) is oscillated at ultrasonic frequency (50-150 kHz) inducing a softening of the metal called acoustic softening effect [3]. This, combined with a high temperature (220°C in our investigated case), softens the material during bonding. Setting up an experiment to characterize the non-linear, plastic behavior would require dedicated equipment with in-situ ultrasonic oscillation capabilities.

Matching at the same time the experimental imposed force and vertical displacement on the capillary is used as a numerical strategy to characterize material for the copper FAB, at high temperature, with a numerical model. In general, stress vs strain curves are obtained for different US powers [3]. After this numerical characterization is done, we can investigate, for example, the effect of different metal schemes below the pad [2]. The ball diameter can also be used as third control parameter. This strategy is valid for experiments with and without acoustic softening.

More than investigating accurately material properties of the copper wire, this paper wants to discuss numerical robustness and approaches that are valid to perform general mechanical simulation with contact and high deformation of domains.

2 The model

As a first step, it was chosen to define the constitutive law of the copper wire at high temperature performing experiments with no US vibration, representing the segments in the actual WB process that do not have it. Three different forces are investigated, 60g ,80g and 100g (Table 1), recording the capillary displacement. The force is the input of the bonding machine while the touch down (TD or displacement) is a recorded output; both can be used as input in the simulation. Given it is a standard nomenclature for the quantity, the force is still reported in grams (g) while it is multiplied by gravity to obtain an actual force (N) when applied in the model.

The piezoelectric actuators that move the capillary have damping and inertia; this means the application of the force is not instantaneous but follows a more complicated law. No information is available on this and both experimental displacements and forces are used, directly as recorded and linearly interpolated, as inputs. Hard experimental pad structure is chosen, thanks to previous experience, allowing us to infer that experimental information contains FAB behavior only.

TD (F 60g)	TD (F 80g)	TD (F 100g)
14.41495659	16.81	20.49917481

Table 1 Capillary displacement (TD) in µm at the different investigated vertical forces. The value is the mean between 5 to 25 ms and on ten wires.

2.1 Model hypothesis

Contact with the default penalty method is used between capillary and ball and ball and pad surfaces. Since the pad can be considered rigid, either a *fixed constraint* on a domain or a meshed surfaced in the *contact pair* can be used; this makes the actual geometry of the pad irrelevant and, given that no US power (horizontal vibration) is present, we can describe our model as 2D axisymmetric. In fact, both ball and capillary can be accurately described as revolution solids (see Figure 3 Geometry of the 2D axisymmetric model). Computational time for the 2D axisymmetric model is in the order of five to ten minutes depending on the details. Several hours of computational time are spared, with respect to 3D, maintaining good accuracy. Moreover, the capillary is also considered un-deformable. No friction is applied, given there is no oscillation. Parametric simulations are mostly performed since inertial behavior is of second order importance and no damping material data are available or investigated in this work. When the capillary is lifted from the ball, this maintains its smashed shape (see Figure 4 Example of ball final shape, this means that *plasticity* is present. A *linear isotropic hardening model* is chosen to describe it. Since only the FAB is deformable and its stress-strain characterization is done at the experimental temperature, no *thermal expansion* is added. Its contribution is already taken into account in the constitutive law.

The mesh can be seen in Figure 5; it is finer on contact surfaces and deformable regions.

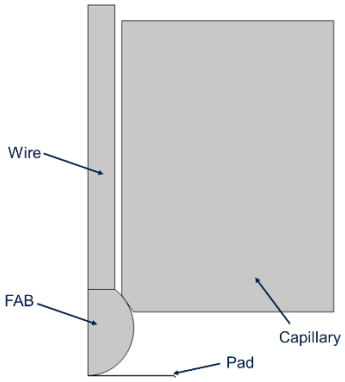

Figure 3 Geometry of the 2D axisymmetric model

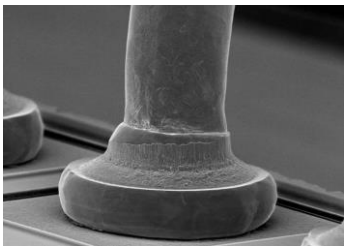

Figure 4 Example of ball final shape

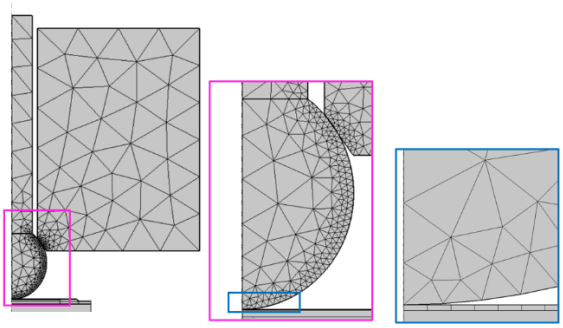

Figure 5 Mesh

2.2 Material properties calibration, displacement controlled

First using the displacement on the capillary as input is investigated. It is imposed through a *rigid material* condition with *prescribed displacement* and increased linearly to match the experimental one of the three forces (see again Table 1).

Material data from literature are taken as starting point (Table 2). The comparison with the experiment is poor; *Young's modulus*, *Initial yield stress* and *isotropic tangent modulus* are parametrically scanned until the force is matched for the three

experimental points (see Figure 6). Proper optimization schemes could be used to improve the matching further.

The validity of the found data is tested against a full bonding curve. The input force is 60g for the first 5 ms and 100 for the remaining 20. These numbers are input of the bonding machine, but actual experimental force and displacement of the capillary are recorded by the machine itself and used in the model. Matching is within 5% when the force is being ramped up while when force is kept constant discrepancy slightly increases (see Figure 8) Regions where the force on the capillary drops to zero are found. This is proof of the numerical accuracy of the force integration on the *rigid material*. Given experimental displacement is not monotone, when the capillary lifts, the ball stays in place due to the occurred plasticity and no force is exerted on the capillary. These regions are not present in the experimental data for the force; this means that some detail is lacking in our physical model. The strongest hypothesis to explain it is found in the lack of description of the kinematic movement of the capillary (which, as it has been shown in [3], requires a lot of data from the experimental machine itself). As a test, monotone displacement is imposed, and we can assess that the above described regions disappear (Figure 8). *Prescribed displacement* only (without the *rigid material condition*) can also be used to control capillary movement. This proves numerically more stable (the computational time halves with the same mesh) without losing numerical accuracy in the computation of the force.

The default Double Dogleg non-linear solver proves robust enough for all above models.

	Initial	After Disp. Calibration
Young Modulus (GPa)	130	80
Poisson's ratio	0.36	0.36
Density (kg/m^3)	8700	8700
Initial yield stress (MPa)	180	50
Isotropic tangent modulus (GPa)	2.1	0.6

Table 2 Copper properties before and after imposed displacement calibration

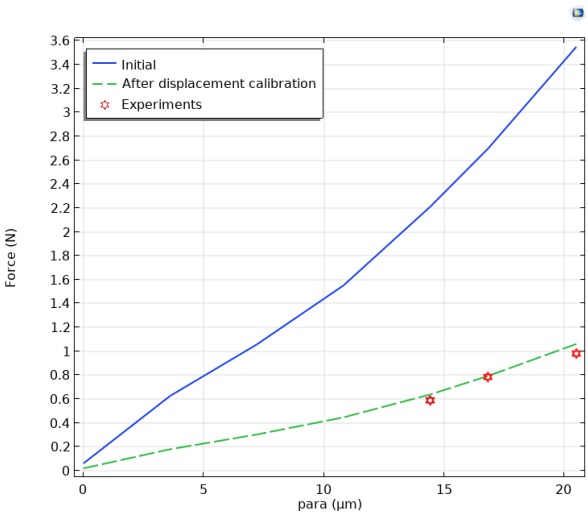

Figure 6 Force (N): initial (continuous-blue), after displacement calibration (dashed-green), red stars: experiment.

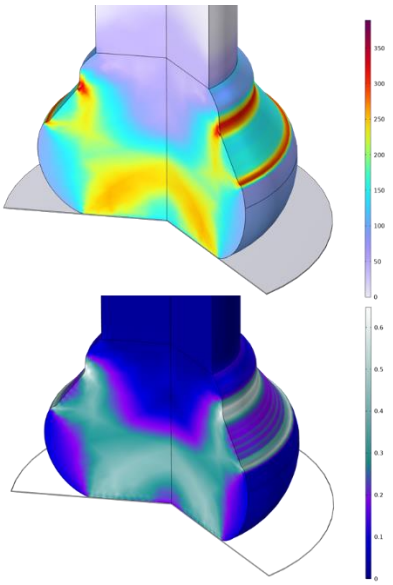

Figure 7 Von Mises stress (MPa), left and plastic strain, right after material calibration and for 100g

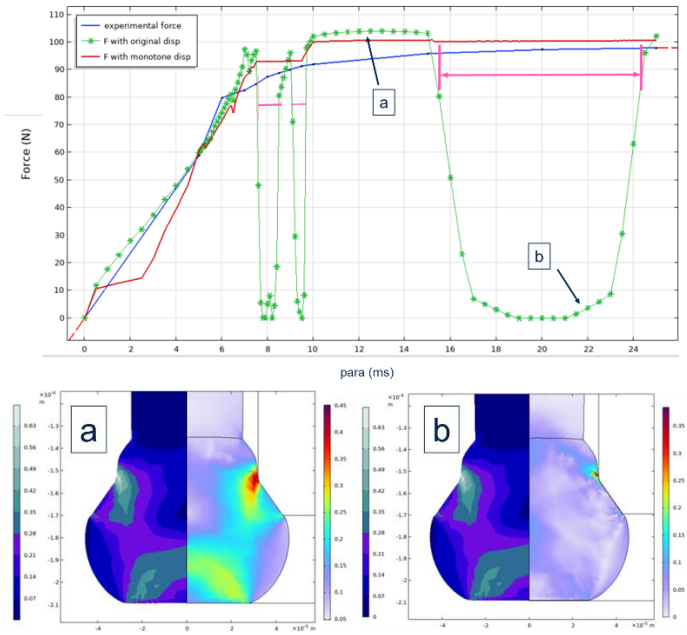

Figure 8 Top: Experimental (blue) and numerical forces (green) with the original displacement. In red the force with monotone displacement. Bottom: Plastic strain left and Von Mises (GPa) right. It can be seen that when the capillary is lifted the stress field is changed but plastic deformation stays in place.

1.1 Material properties calibration, force controlled

In the previous chapter the displacement was used as an input for the model and the force as the control variable, now the opposite is done. In principle, both strategies should provide the same results, but this is true only if the physics of the system is fully understood. As mentioned, at least the kinematic behavior of the piezoelectric capillary actuator would be needed to try and converge these two approaches.

Before commenting on the results, a little digression is needed on constraints. When the force is imposed on the

capillary, in static simulation, a constraint is missing in the vertical direction (in 2D axisymmetric no rotation is possible and a constraint in r is provided by the axis itself). To resolve this an *initial interference* between capillary and ball is used (see Figure 9). This interference is resolved by the software at step zero; it allows for a less cumbersome set up and analysis of the results of the model with respect to the use of spring foundations.

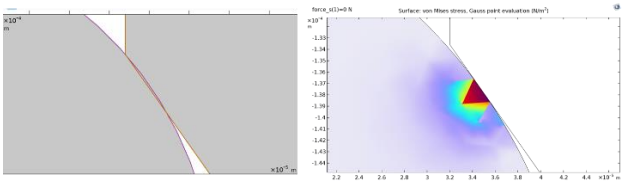

Figure 9 Geometrical interference (left), solution at para=0 (right).

Both for the three forces and the whole calibration curve displacements are obtained (Figure 10), showing a 15% discrepancy with the experimental displacement. We can also appreciate the difference between the final shapes of the ball between the two strategies (Figure 11).

A second calibration is then performed with the whole curve and a change in *isotropic tangent modulus* to 0.5 GPa is found to match the result better (Figure 12).

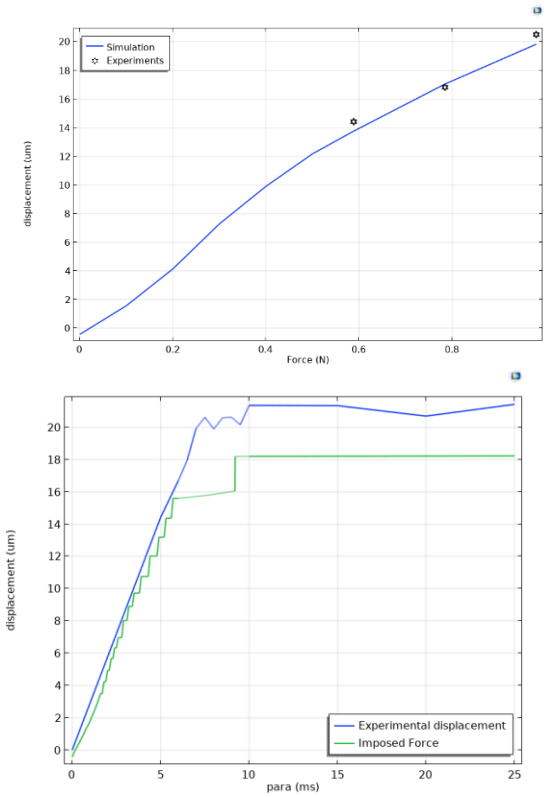

Figure 10 Top: the static calibration (experimental points in black). Bottom: the comparison on a whole bonding segment.

The same material data are then re-used with *prescribed displacements* (Figure 13). As commented before, the two approaches are only equivalent in theory since the physic is not described in enough details. We can see that with the same material data that properly match the TD imposing the force, overestimation of the force is observed imposing the TD.

To make the computations more robust when using the force as input, non linear solver is changed from the default Double Dogleg to the more 'cautious' *constant Newton* with 0.1 as damping factor.

Imposing the displacement is in general more robust (i.e. faster computational times) and should be preferred when the choice is possible.

A transient simulation (Figure 14) is also performed and seems to more accurately, but not perfectly, capture the experimental behavior. More investigation is needed to verify this finding.

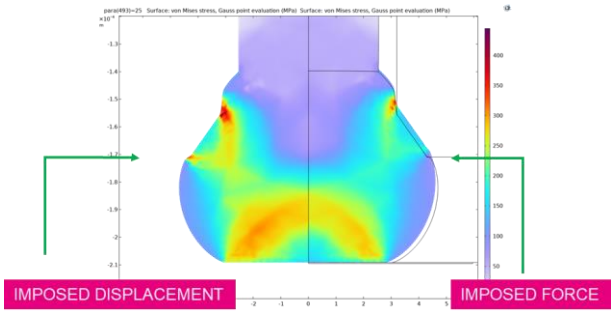

Figure 11 Final deformation for whole segment simulation (Von Mises Stress, MPa)

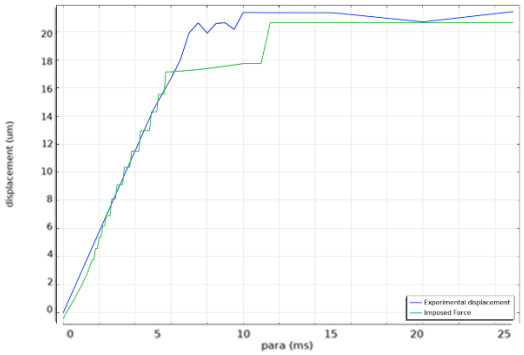

Figure 12 Displacement, numerical vs experimental with isotropic tangent modulus of 0.5 GPa

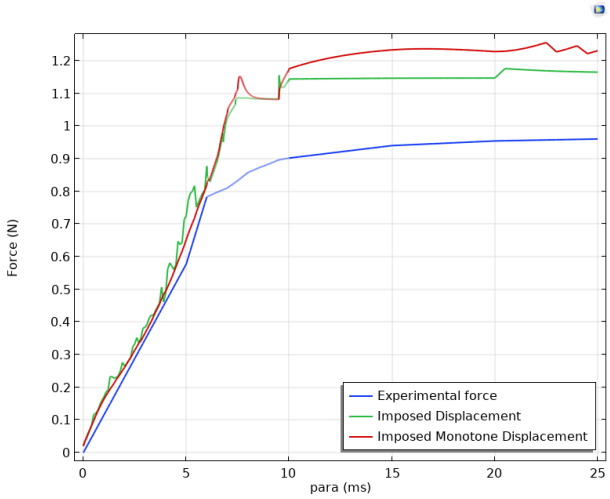

Figure 13 Experimental vs. numerical force with isotropic tangent modulus 0.5 GPa

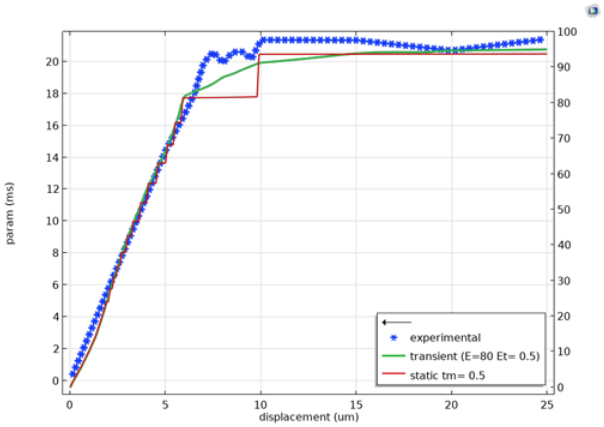

Figure 14 Transient (green) vs parametric (red) simulation

1.2 Further points of discussion

First steps toward a robust model set up are also made both for static and transient 3D analysis. 3D is not only slower but more critical with respect to constraints to be imposed, computational time and robustness. It is, in any case, fundamental toward building a predictive model (including USV and pad actual geometry). Beside vertical displacement, in the z coordinate, (or interference if the force is imposed) both FAB (at the top) and capillary need to be constrained in plane. The in-plane capillary movement is zero in the case of no acoustic softening.

Deformation of the ball is low when no acoustic softening is present, this means that a *linear elastic with plasticity* description is robust enough to accommodate the deformation. In ongoing simulations, that are not described in this paper, where no US power is present, this model proved too poor to correctly describe the stress-strain behavior of the copper wire; a *Ludwik model* is more apt to describe it.

When US vibration is present, the material is significantly softer and the ball deformation is much higher. *Neo Hookean Hyperplastic model* is used to make such simulation more numerically stable, especially in 3D. The default *quadratic discretization* should be maintained given the more robust and cheaper linear one is not able to capture the ball shape correctly (see Figure 15).

Coming to *transient simulations*: if the physics contains inertial terms, there is no need for constraints (interference) or spring foundations for the problem to be mathematically well posed. On the other hand, material damping information would be needed to build a physically sound model. Since no information on material damping is available the *BDF time stepping solver* is used for our transient tests, instead of the default generalized alpha, to introduce numerical damping.

If then the pad is considered not rigid and *initial strains\stresses* are introduced in some layers, even more care should be put into defying constraints. In fact, if the FAB is unconstrained vertically and touches the pad it may move at t (or para) =0. This is because there will be an initial deformation of the below layers that displaces it.

Thermal stress should also be introduced.

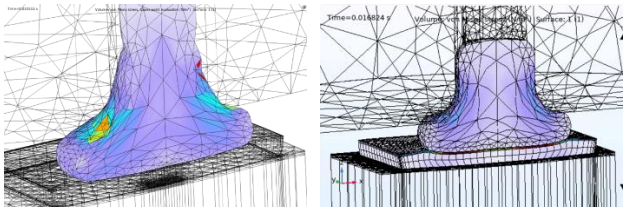

Figure 15 Shape of the ball, linear vs. quadratic elements

3.0 Conclusion & future investigations

We have seen how numerical simulations, combined with experimental data, can be used to infer material properties when specific characterization is missing or unfeasible, reaching a good degree of accuracy.

Displacement controlled and force controlled capillary movement produce slightly different results given the kinematic behavior of the piezoelectric actuator is unknown.

Displacement is, as expected, to be preferred as more robust numerical input over force. Some insights to 3D and transient models are provided.

Further enhancements could be to model ball-pad adhesion and, when acoustic softening is present, to control the horizontal capillary displacement imposing a force, allowing for oscillation amplitude damping due to weld formation.

References

1. G. Harman ‘Wire bonding in microelectronics’, third edition, chapter 1.
2. L. Guarino et al, ‘Hard bond pad plastic deformation study for adhesion estimation by 3D FEM modelling of wire bonding process’2023 IEEE 25th Electronics Packaging Technology Conference (EPTC)
3. Amir Siddiq et al., Acoustic softening in metals during ultrasonic assisted deformation via CP-FEM, *Material Letters,* October 2010.
4. A Shah et al, ‘Ultrasonic friction power during thermos-sonic Au and Cu ball bonding’, Journal of Physics D: Applied Physics, Volume 43, Number 32